# Demonstration of a Cryogenic Boil-Off Reduction System Employing an Actively Cooled Thermal Radiation Shield

**J. R. Feller[1], D. W. Plachta[2], G. Mills[3], and C. McLean[3]**

[1]NASA Ames Research Center
Moffett Field, CA, USA

[2]NASA Glenn Research Center
Cleveland, OH, USA

[3]Ball Aerospace Technologies Corporation
Boulder, CO, USA

## ABSTRACT

NASA, under the Cryogenic Fluid Management (CFM) Project, in partnership with Ball Aerospace Technologies Corporation (BATC), conducted a reduced boil-off demonstration employing an actively cooled thermal radiation shield. The shield, designed and fabricated by NASA, consisted of overlapping panels of 1100 aluminum foil, and three parallel 1/8 inch cooling lines attached to the foil with adhesive and communicating with 1/4 inch inlet and outlet manifolds. The shield and gas distribution network were instrumented and integrated with BATC's 500 L liquid nitrogen (LN2) cryogenic propellant tank simulator, high-performance multi-layer insulation (MLI), and a cryocooler and pressurized helium circulator. Two test conditions were run to evaluate the thermal performance of the system. An initial test was performed to measure the baseline or passive steady state heat leak into the LN2 tank. In the second test, the cryocooler/circulator was driven at maximum power until the system again reached steady state. By removing heat from both the shield and the tank support structure via the circulating helium stream, the average shield temperature dropped from ~228 K to ~132 K and the total heat leak into the tank was reduced by 82 %. This was despite the fact that the flow rate in the distribution network was unexpectedly low due to a partial blockage in one of the recuperators.

## INTRODUCTION

Between 2004 and 2006, NASA, under the In-Space Cryogenic Propellant Depot (ISCPD) Project[1], investigated various options by which cryocoolers might be integrated with cryogenic propellant storage tanks. The goal was to substantially reduce or entirely eliminate boil-off losses without prohibitively increasing total system mass. For liquid oxygen (LO2) storage, the solution is straightforward in principle, as it is possible to integrate existing high capacity 90 K flight coolers, or derivations of them, directly with an LO2 tank. But for liquid hydrogen (LH2) storage, this is not a viable option because the required 20 K coolers do not yet exist. However,

*Cryocoolers 16,* edited by S.D. Miller and R.G. Ross, Jr.

the analysis performed under ISCPD predicted that a large percentage of the heat leak into an LH2 tank could be intercepted at ~90 K, thus circumventing the need for a high capacity 20 K flight cryocooler. Thus came about the broad area cooling (BAC) concept, whereby heat is removed, via a pressurized helium circulation network, from a large but low-mass metal foil thermal radiation shield embedded within an LH2 tank's passive thermal insulation system. Analytical tools and models were developed[2,3] and eventually incorporated into a general cryogenic system analysis software package, with which a series of trade studies was conducted.[3] These trades determined practical ranges of values for the circulation loop charge pressure, mass flow rate, tubing diameter, and foil thickness, based on likely mission scenarios.

In order to advance the technology readiness level (TRL) of this concept, the Cryogenic Fluid Management (CFM) Project funded, in addition to the ongoing analytical/modeling effort, a series of three experiments[4,5,6] at NASA Ames Research Center (ARC) designed to investigate questions of thermal control stability, heat transfer effectiveness, and temperature uniformity in distributed cooling systems. The overall TRL has consequently been raised from 3 to 5.

Subsequently, under its Innovative Partnership Program (IPP), NASA partnered with Ball Aerospace Technologies Corporation (BATC) to implement and demonstrate the BAC shield concept on a system level. The resulting test program is the subject of this paper.

## THE REDUCED BOIL-OFF EXPERIMENT

### Primary Test Components

**Dewar, Multi-Layer Insulation, and Cryocooler.** The objective of the test program was to characterize the thermal performance of an actively cooled BAC shield, which was embedded within the multi-layer insulation surrounding the BATC 500 L liquid nitrogen (LN2) test tank (a propellant tank simulator), and integrated with the BATC SB235E two-stage Stirling cryocooler.

The BATC high-performance MLI that had been installed on the tank for a previous test program consisted of ten sub-blankets. For this test, the fourth (counting from the tank wall) sub-blanket was removed in order to accommodate the NASA shield. In all there were 12 layers of double-aluminized Mylar between the tank wall and the active shield and 24 between the shield and the room temperature thermal environment of the vacuum chamber. Nominally, the MLI above and below the shield was identical, except for thickness. However, as discussed below, it is evident that the presence of the shield resulted in unequal compressions of the two blankets, thus adding some indeterminacy to the heat leak calculations.

The tank and shield were suspended from the vacuum chamber lid by three identical symmetrically located 0.5 in. diameter 4301L Torlon® rods. This material was chosen for its high strength and low thermal conductivity.

**The Actively Cooled Shield.** The actively cooled shield (Fig. 1) was composed of seven 1100 aluminum foil panels. Its shape and dimensions were dictated by those of the existing MLI. The three side panels, which formed the central cylindrical section of the shield, were 5 mil in thickness. Running vertically down the center of each was an 1/8 in. OD stainless steel cooling tube. The tubing was bonded to the foil using Loctite® Hysol® 9430, a modified epoxy adhesive, which was chosen because of its reportedly high peel and shear strength, and its flexibility at room temperature. These are desirable qualities because of the thermal expansion mismatch between the tubing and foil.

The top and bottom end caps of the shield were constructed from flat 15 mil sheets. When assembled they formed truncated cones. The circular inlet and outlet gas distribution manifolds, made from 1/4 inch stainless steel tubing, were simply attached using aluminum tape. Three slots were cut into the top conical section to allow installation without disconnecting the tank from the chamber lid. The split top disk with the central hole was installed around the tank fill/vent line. Aluminum straps linked the top conical panel with the Torlon rods; these links were both mechanical (supporting the entire shield as well as the overlying MLI) and thermal, thus intercepting a portion of the conductive heat leak.

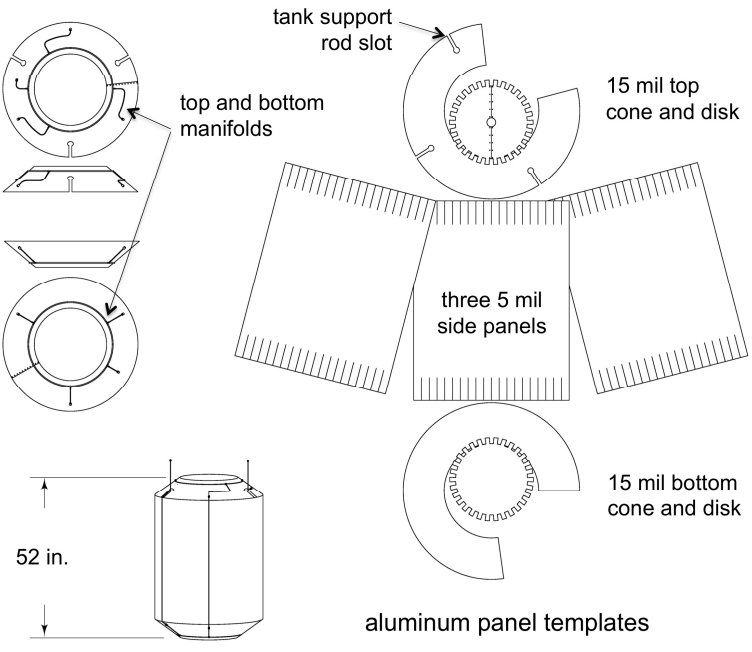


**Figure 1.** The actively cooled thermal radiation shield, constructed from flat 1100 aluminum panels.

When fully assembled, the side panels overlapped each other by ~2 inches but were not attached. The flaps at the top and bottom of the side panels were folded over the conical sections and riveted. The tubing sections were connected to each other with 1/8 inch VCR fittings. The inlet and outlet manifolds were connected to the cryocooler/circulator ports by 1/4 inch OD stainless steel tubing. These lines were each wrapped in ten layers of aluminized Mylar.

The height of the assembled shield, from the bottom to the top disk, was ~52 inches; the diameter of the cylindrical section was ~35 inches.

**Measurements.** All cryogenic temperature measurements were made using silicon diode thermometers (SDTs). Seven SDTs were dedicated to the shield itself: one on each of the top and bottom circular panels; one on the top conical section, adjacent to the attachment point of one of the structural/thermal straps; one at the center of each side panel, adjacent to the vertical cooling lines, and one near the edge of one of the panels, midway between two of the cooling lines. The distributed cooling network was further instrumented with SDTs mounted on heat exchangers at the cryocooler/circulator inlet and outlet; these gave the total $\Delta T$ across the network.

The tank wall temperature was measured at two points: on its bottom dome and top dome (near the connection point of one of the Torlon rods). In order to characterize the conduction heat leak through the tank supports, one of the three identical rod/strap assemblies was instrumented with four SDTs: at the top of the Torlon rod; at the top dome of the tank (already noted above) adjacent to the Torlon rod connection point; on the aluminum clamp linking the strap to the Torlon rod; and on the shield top conical section (also noted above) adjacent to the strap attachment point. Thus the $\Delta T$s between the top of the Torlon rod and the aluminum strap, between the aluminum strap and the tank wall, and across the strap between the Torlon rod and the shield, were all measured.

Pressures sensors were placed on the inlet and outlet ports of the circulator, thus giving the total network $\Delta P$, including the cold head heat exchangers and the two recuperators. Finally, the

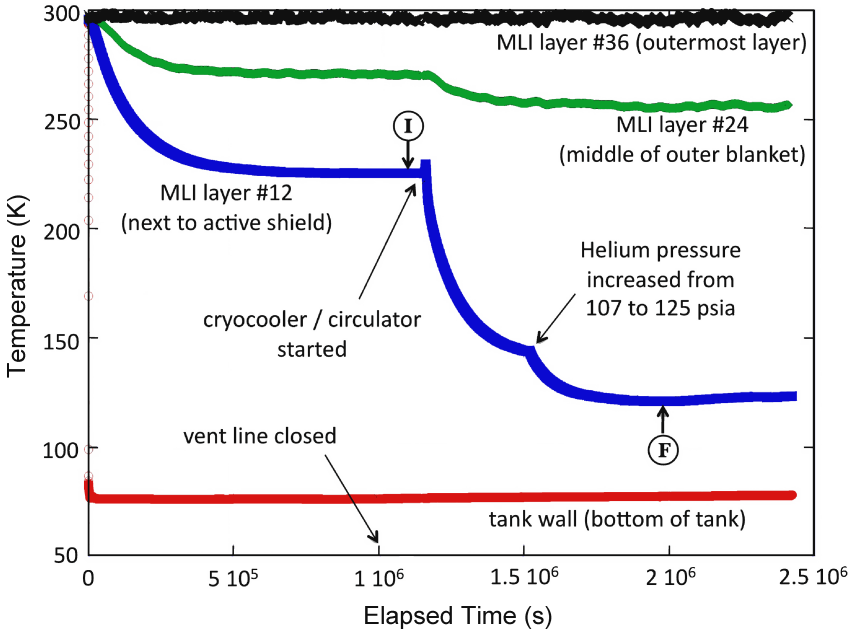


**Figure 2.** Some representative system temperatures, plotted over the entire three-week run.

tank pressure was measured. This, along with the tank wall temperature, allowed the total heat leak into the tank to be calculated.

**Test Overview and Summary of Major Events**

Some representative system temperatures are plotted vs. elapsed time (from test start to finish) in Fig. 2. The tank wall was close to 77 K and the outer MLI layer was near room temperature. The twelfth MLI layer was adjacent to the actively cooled shield and closely tracked its temperature. Also shown is the temperature in the middle of the outer MLI blanket.

The duration of the test was ~28 days. Time $t = 0$ is defined as the beginning of the first LN2 transfer (start of the cool-down). The system required ~11.5 days to reach steady state. At this time (indicated in Fig. 2) a final LN2 transfer was performed, bringing the tank to 95% fill level, and the vent valve was closed. The cryocooler/circulator was started about 13 days into the test. After four days of operation the helium pressure in the circulation loop was increased (at the indicated point), allowing the drive frequency of the cooler's compressor to be increased from 40 to 44 Hz. This was done to increase the thermal capacity of the helium stream, thus resulting in a lower shield temperature in the final steady state.

A small leak (*not* into the vacuum chamber) caused a gradual loss of pressure in the circulation loop. This accounts for the slight temperature rise towards the end of the test.

Two test conditions were run to evaluate the thermal performance of the system. An initial test (at time labeled *I* in the figure) was performed to measure the baseline or passive steady state heat leak into the LN2 tank. In the second or final test (labeled *F*, at which time the shield temperature was at a broad minimum), the cryocooler/circulator were driven at maximum power until the system again reached steady state (actually a quasi-steady state due to the leak). Both tests were performed with the tank vent line closed. The heat leak calculations were based on the temperature and pressure rise rates of the LN2, instead of the flow rate of the boil-off as would be the case in a vented tank calorimeter.

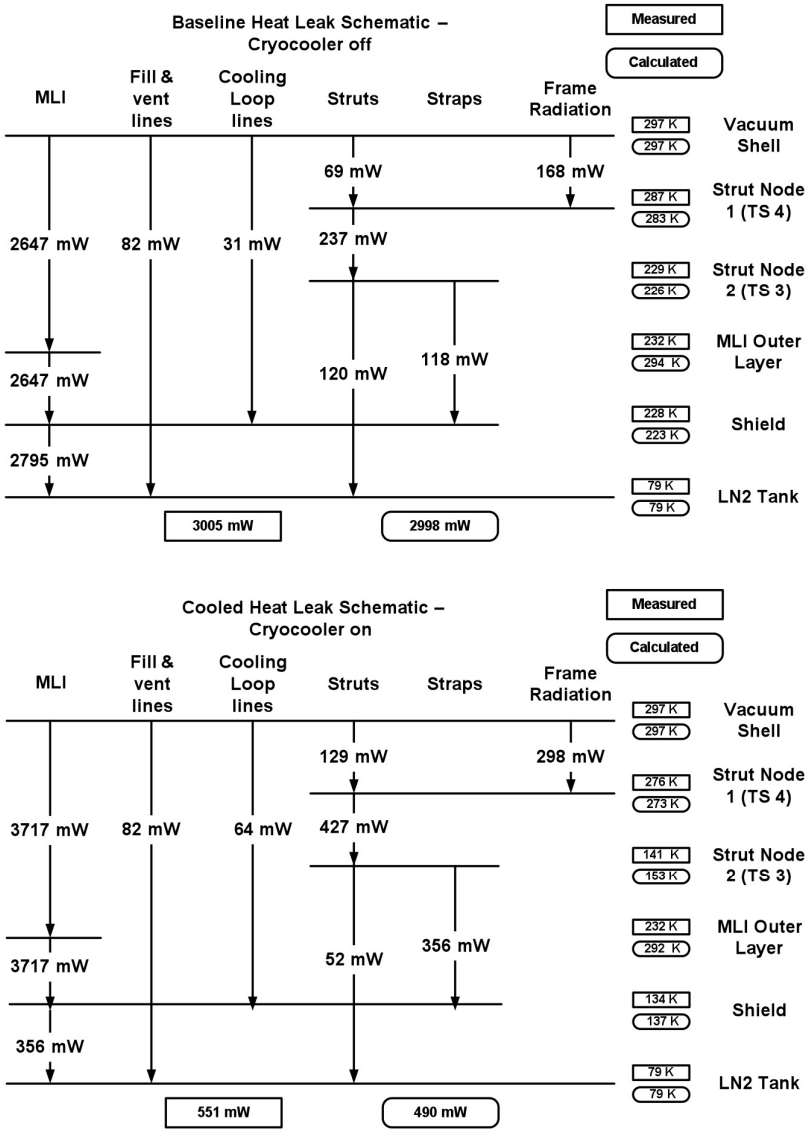


**Figure 3.** Results of a TAK (SINDA) thermal model of the system. Top: Initial or baseline steady state (cryocooler/circulator off). Bottom: Final steady state (cryocooler/circulator driven at maximum power).

## Test Data and Heat Leak Analysis: Initial and Final Steady States

The tank temperature and pressure were measured and recorded throughout testing, allowing the internal energy of the LN2 to be calculated. For LN2 properties, NIST REFPROP was consulted. The rate at which the internal energy increased then gave the total heat leak into the tank in the initial and final steady states (3.00 W and 0.55 W, respectively).

The "waterfall" charts in Fig. 3 summarize the results of a six-node TAK (SINDA) thermal model based on the known hardware dimensions and thermal properties. Strut nodes 1 and 2

refer, respectively, to the top of the Torlon rod and the top of the aluminum strap (where it is clamped to the rod). All three rod/strap assemblies have here been lumped together.

As noted above, the effective conductance of the underlying and overlying MLI blankets were somewhat indeterminate due to compression. These were varied (within reason) to give a best fit to the measured temperatures and the total heat leak into the tank. Not shown explicitly in Fig. 3 is the heat removed from the shield. This is found simply by calculating the energy imbalance at the shield node.

The value of this analysis is that: (1) The total heat leak into the tank has been broken down into components, namely MLI, fill and vent lines, and support structure; and (2) the net heat load on the shield is determined and has also been broken down into three components, which are the MLI, the inlet and outlet lines (labeled cooling loop lines), and the heat load intercepted at the support rods.

## PERFORMANCE OF THE ACTIVELY COOLED SHIELD

### Mass Flow Rates and Pressure Drop in the Distributed Cooling Network

The design of the BAC shield was based on the expected net heat load and total mass flow rate. The expected net heat load on the shield (3 to 4 W) was more or less on target. If the cryocooler/circulator had delivered the expected flow rate of ~100 mg/s or more then the maximum $\Delta T$ on the shield would have been less than 4 K (as opposed to nearly 11 K), the total network $\Delta T$ would have been around 9 K (as opposed to nearly 37 K), and the system would have cooled down significantly faster. However, due to a partial blockage in one of the recuperative heat exchangers, the total mass flow rate was initially only ~17 mg/s. This was increased, as alluded to above, to ~23 mg/s. In the final steady state the total mass flow rate was $\dot{m}$ = 22.77 mg/s, so that the flow rate in each of the three branches was ~7.6 mg/s (ignoring for the moment mismatches in flow impedance).

In the final steady state, the total pressure drop between the outlet and inlet of the helium circulator was only 20.3 psi, and presumably the better part of this was across the recuperators.

### Heat Transfer Rates in the Distributed Cooling Network

The total heat removed from the distributed cooling network is simply given by[8]

$$\dot{Q}_{total} = \dot{H}_{out} - \dot{H}_{in} = \dot{m} c_p (T_{out} - T_{in}) = \dot{m} c_p \Delta T_{stream}, \quad (1)$$

where $\dot{H}_{in}$ is the enthalpy flow rate of the gas stream at the network inlet, $\dot{H}_{out}$ is the enthalpy flow rate at the outlet, $T_{in}$ and $T_{out}$ are the corresponding gas stream temperatures (taken to be equal to the measured inlet and outlet heat exchanger temperatures), $\dot{m}$ is the total mass flow rate, and $c_p$ = 5190 J/Kg·K is the mass-specific heat of the helium, which is approximately constant. In the final steady state $T_{in}$ = 106.54 K, $T_{out}$ = 143.37 K, and $\Delta T_{stream}$ = 36.83 K. So $\dot{Q}_{total}$ = 4.35 W.

Most of this heat is transferred to the distribution network from the shield, as was to be expected. Applying conservation of energy to the shield node in Fig. 3 (bottom) it is found that the net heat load on the shield is $\dot{Q}_{net}$ = 3.78 W. This must be equal to the heat removed via the helium stream. The difference $\dot{Q}_{total} - \dot{Q}_{net}$ = 570 mW must be considered parasitic, most likely the combined radiative heat load on the inlet and outlet lines. In fact a rough calculation based on the line lengths and temperatures, the vacuum chamber temperature, and the number of layers (ten) of aluminized Mylar insulating the lines yields ~0.6 W.

### Thermal Gradients

**Temperature Rise in the Cooling Lines.** As stated in the previous section, the total temperature rise of the helium stream between the inlet and outlet of the distribution network is $\Delta T_{stream}$ = 36.83 K, corresponding to the total heat load $\dot{Q}_{total}$ = 4.35 W. Of this 570 mW is

parasitic. The corresponding temperature rise is found by dividing by $\dot{m}c_p$, which gives $\Delta T_{par}$ = 4.85 K. Then the temperature rise of the stream between the inlet and outlet of the shield itself is 31.98 K.

**Temperature Rise in the Shield Parallel to the Cooling Lines.** This is $\Delta T_{//}$ = 10.2 K, the difference between the temperature of the top of the shield (137.27 K) and the bottom of the shield (127.07 K). If there were no other heat transfer path between these points aside from the helium stream then one would expect $\Delta T_{//}$ to be equal to $\Delta T_{stream}$. However, the foil shield itself provides a parallel conduction path, as does the surrounding MLI. The in-plane thermal conductivity of the MLI evidently has a significant ameliorative effect on the shield temperature non-uniformity. This effect had not previously been taken into account.

**Temperature Rise in the Shield Perpendicular to the Cooling Lines.** One of the side panels was instrumented with two SDTs, one directly adjacent to the cooling line and the second near its edge, a distance $w/2$ from the cooling line, where $w$ is the circumferential inter-line spacing (the shield circumference divided by three). The measured temperature rise between these two points is $\Delta T_{\perp}$ = 1.9 K. The theoretical value is[6]

$$\Delta T_{\perp} = \dot{q}_{net} w^2 / 8\kappa_{shield} t, \tag{2}$$

where $w$ = 0.925 m, $t$ = 5 mil is the shield thickness, $\kappa_{shield}$ = 225.5 W/m·K is the NIST value for the thermal conductivity of 1100 aluminum at the shield temperature, and $\dot{q}_{net} = \dot{Q}_{net} / A_{shield}$ is the net heat flux on the shield, or the net heat load divided by the total surface area (4.3 m$^2$) of the shield. The theoretical value is found to be 3.3 K, which is not insignificantly higher than the measured value. This is another indication of the ameliorative effect of the surrounding MLI.

**General Observations.** Two SDTs were mounted on the top sections of the shield: on the circular section and near the lower edge of the conical section. In the final steady state the difference between these temperatures was only 0.59 K, which is not surprising given the thickness (15 mil) of the aluminum.

The central temperatures of the three 5-mil side panels were 130.4 K, 129.99 K, and 128.05 K, which may suggest that the flow rate through the third branch was slightly higher than in the other two. This imbalance is by no means dramatic.

The largest measured $\Delta T$ on the shield was 10.79 K. This is surprisingly small given the much lower than expected flow rate in the cooling loop.

### Metrics of the Active Shield's Thermal Performance

The most obvious measure of the effectiveness of the actively cooled shield is the relative reduction in heat leak: $\Delta\dot{Q}/\dot{Q}_{tank,passive}$ = .82, where $\Delta\dot{Q} = \dot{Q}_{tank,passive} - \dot{Q}_{tank,active}$ = 2.45 W.

If something more like a gain to expenditure ratio is desired, then it is natural to consider the quantity

$$\eta_S = \frac{\Delta\dot{Q}}{\dot{Q}_{net}}. \tag{3}$$

Comparing the initial and final steady states, $\eta_S$ = 0.65. This ratio behaves like a thermal effectiveness (it will be referred to as the shield effectiveness). In general practice it would vary from 0 to 1. It approaches 0 for $\dot{Q}_{net} >> \Delta\dot{Q}$, which clearly represents a very ineffective system, and equals 1 only when $\Delta\dot{Q} = \dot{Q}_{net}$, which would be the best that one could possibly hope to achieve.

If there are no thermal shorts between the warm and cold boundaries of the MLI, that is, if heat is transferred only through the MLI (from the warm boundary to the active shield, and from the active shield to the cold boundary) or out through the circulation loop, then it is easy to show[8] that

$$\eta_S = \frac{N-k}{N-1} \quad \text{(no thermal shorts)}, \tag{4}$$

where $N$ is the total number of layers in the MLI, with the active shield counted as the $k^{\text{th}}$ layer. This also assumes that the heat flux from some layer $n$ to another layer $m < n$, both within a continuous MLI blanket (all layers passive), can be expressed in the form

$$\dot{q}_{n\to m} = \frac{L(T_n, T_m)}{n-m}, \tag{5}$$

where $L(T_n, T_m)$ depends explicitly only on the boundary temperatures $T_n$ and $T_m < T_n$, and furthermore that $L$ is a sum of terms of the form $C\cdot\left(T_n^{\alpha} - T_m^{\alpha}\right)$, where $C$ and $\alpha$ are constant within the blanket. This is not terribly restrictive, as the various "Lockheed equations," first developed by Cunnington, *et al.*[9], and now widely in use, are of this form.

Judging from Eq. (4), the shield effectiveness is not very informative. It simply says that if one wishes to intercept *all* of the heat leak, then the best place to do it is at the cold boundary where the actively cooled shield would be best isolated (by the entire MLI blanket) from the warm boundary. Conversely, the worst place to do it is at the warm boundary. Nevertheless, Eqs. (3) and (4) do provide a simple verification of the system thermal analysis discussed earlier.

Returning to the test system, the total number of shields (both passive and active) between the warm and cold boundaries is $N = 37$, and layer $k = 13$ is the actively cooled shield. So the ratio $(N-k)/(N-1)$ is 0.67, which is close to the shield effectiveness 0.65 calculated using Eq. (3). This should not be too surprising, as the heat leak through the MLI dominates the total heat leak into the LN2 tank. Still, Eq. (4) is not strictly correct, as there are thermal shorts (*e.g.*, the tank support rods, etc.). However, if all the heat leaks through the thermal shorts are properly subtracted from $\Delta\dot{Q}$ and $\dot{Q}_{net}$ then the resulting ratio, which should now theoretically be equal to the ratio in Eq. (4), takes on the value 0.68. Thus the corrected correspondence between Eq. (3) and Eq. (4) is remarkably good.

A third and final metric is perhaps more useful, and is more orthodox in its definition. Define the thermal effectiveness ratio

$$\varepsilon = \frac{\dot{Q}_{net}}{\dot{Q}_{net} + \dot{Q}_{tank}} = \left(1 + \frac{\dot{Q}_{tank}}{\dot{Q}_{net}}\right)^{-1}, \tag{6}$$

where $\dot{Q}_{tank}$ is the total heat leak into the tank. Clearly, $\varepsilon \to 0$ as $\dot{Q}_{net} \to 0$ (no heat is removed from the system, so the shield is totally ineffective) and $\varepsilon \to 1$ as $\dot{Q}_{tank} \to 0$ (there is no heat leak to the tank, so the shield is totally effective). In the final steady state, $\varepsilon = 0.89$.

Of course a true measure of the *system* performance would have to include the efficiency of the cryocooler/circulator and the heat transfer effectiveness of every heat exchanger. That, however, is beyond the scope of this study.

## ACKNOWLEDGMENT

This work was partially funded by NASA's Cryogenic Fluid Management (CFM) Project, under the Exploration Technology Development Program (ETDP).

## REFERENCES

1. "In-Space Cryogenic Propellant Depot (ISCPD) Project," funded by the NASA Headquarters Exploration System Research and Technology (ESR&T) Division of the Office of Exploration Systems.
2. Feller, J.R., Salerno, L.J., Kashani, A., Helvensteijn, B.P.M., Maddocks, J.R., Nellis, G.F, and Gianchardani, Y.B., "Technologies for Cooling of Large Distributed Loads," *Proceedings of the AIAA Space 2008 Conference & Exposition*, American Institute of Aeronautics and Astronautics (2008).
3. Plachta, D.W., Christie, R.J., Carlberg, E., and Feller, J.R., "Cryogenic Propellant Boil-Off Reduction System," *Advances in Cryogenic Engineering*, AIP, New York (2008), p. 1457.

4. Feller, J.R., Kashani, A., Helvensteijn, B.P.M, and Salerno, L.J., "Summary of Distributed Cooling and Advanced Regenerator Test Fixture Development," Report to the NASA CFM Project (2008), unpublished.

5. Feller, J.R., Salerno, L.J., Kashani, A., Maddocks, J.R., Helvensteijn, B.P.M, Nellis, G.F., and Gianchardani, Y.B., "Distributed Cooling Techniques for Cryogenic Boil-Off Reduction Systems," *Cryocoolers 15,* Kluwer Academic/Plenum Publishers, New York (2009), pp. 631-635.

6. Feller, J.R., Kashani, A., Helvensteijn, B.P.M, and Salerno, L.J., "Characterization of an Actively Cooled Metal Foil Thermal Radiation Shield," *Adv. in Cryogenic Engineering*, Vol. 55, Amer. Institute of Physics, Melville, NY (2010), pp. 1187-1194.

7. Feller, J.R., Kashani, A., Helvensteijn, B.P.M, Salerno, L.J, Kittel, P., Plachta, D., Christie, R., and Carlberg, E., "Analysis of Continuous Heat Exchangers for Cryogenic Boil-Off Reduction," *Adv. in Cryogenic Engineering*, Vol. 53, Amer. Institute of Physics, Melville, NY (2008), pp. 401-408.

8. Feller, J.R., Salerno, L.J., Kashani, A., and Helvensteijn, B.P.M, "Summary of Distributed Cooling Design and Analysis Tools for Cryogenic Fluid Management Applications," Report to the NASA CFM Project (2009).

9. Cunnington, G.R., Keller, C.W., and Bell, G.A., "Thermal Performance of Multi-Layer Insulations–Interim Report," NASA-CR 72605 (1971).